Numerical Computation of a Stationary Two-Dimensional Vortex Flow in the Presence of a Barrier

ROBERT R. HWANG, H. P. PAO and T. Y. KOU

Institute of Physics, Academia Sinica
Nankang, Taipei, Taiwan

(Manuscript received 10 January 1977, in revised form 12 March, 1977)

ABSTRACT

In this study effect of barrier on the vortex is studied theoretically in terms of the understanding of the dynamical events associated with its blocking phenomena. A numerical model has been successfully developed for a stationary two-dimensional vortex flow in the presence of a barrier, using the full Navier-Stokes equations. The numerical results show the development of flow separation in the lee of the barrier and its formation of a secondary vortex behind the barrier. These results were compared favorably to the laboratory experiments and the field data on typhoons when encountering the island of Taiwan.

1. Introduction

The importance of topographic effects on the atmospheric flows has led to numerous studies and investigations by many scientists throughout the world in recent years. Although it has been recognized that mountain ranges have strong interaction with and influence over typhoons, the problem of studying the dynamics of a typhoon vortex in the presence of barriers seems to have not been very well investigated. In order to reduce human and economic losses resulting from typhoons, it is important to understand the phenomena and mechanism of the block effect when a typhoon vortex is in the vicinity of mountain barriers. With the strong two dimensional characters assured by its high rotational intensity, typhoon can be treated as a quasi-two-dimensional rotationally constrained fluid and considered as a two-dimensional concentrated vortex. This paper is then to study the flow pattern of a uniform flow associated with a fixed vortex in the presence of a barrier.

The literature on the flow past obstacles is extensive. The survey papers by Morkovin (1964), Krzywoblocki (1966) and Berger & Wille (1972) should be mentioned. They studied the onset and the process of vortex shedding behind bodies which are positioned symmetrically relative to the main flow. Recently, Lugt & Haussling (1974) investigated theoretically the process of generation and shedding of the initial vortex for laminar incompressible fluid flows past an abruptly started elliptic cylinder at 45° incidence for Reynolds number from 30 to 300. However, the form and the onset of induced vortex behind barriers in the combinations of uniform flow and a fixed vortex for both symetric and asymetric flows are not well understood. In this paper, two cases of time-dependent laminar flow associated with a fixed vortex in the upstream of a two-dimensional elliptical barrier are considered. A numerical finite-difference scheme for the stream-function/vorticity formulation is used to study the dynamic behavior of such flow conditions. Results of the numerical computations are compared to the laboratory experiments and the field data on typhoons when encountering the island of Taiwan.

2. The Flow Problem

The developing flow due to a uniform flow associated with a fixed vortex in the upstream of a two-dimensional elliptical barrier in an open incompressible fluid is considered and shown in Fig. 1. Mathematically an initial/boundary-value problem for the two-dimensional

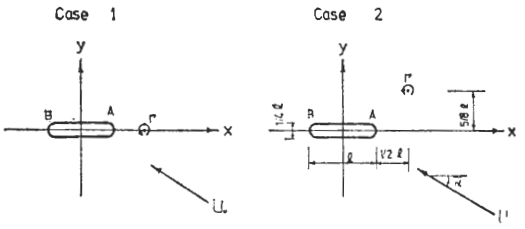

Fig. 1. Schemetic diagram of flow problems.

Navier-Stokes equations with appropriate initial and boundary conditions, must be solved to the flow problem. These equations are conveniently carried out in the dimensionless form. In order to non-dimensionalize the variables, we introduce the characteristic length, time and velocity to be ℓ, ℓ^2/Γ' and Γ'/ℓ respectively, where ℓ is the length of the elliptical cylinder and Γ' the circulation of the fixed vortex divided by 2π. The dimensionless variables are then defined as

$$u^*=u/(\Gamma'/\ell),\ v^*=v/(\Gamma'/\ell),\ x^*=x/\ell,$$
$$y^*=y^*/\ell,\ t^*=t/(\ell^2/\Gamma'),\ \psi^*=\psi/\Gamma',$$
$$\zeta^*=\zeta/(\Gamma'/\ell^2) \qquad (1)$$

In terms of these and neglecting the asterisk symbol on the superscript of varibles, the equations of motion are formulated in forms of the dimensionless stream function ψ and ζ, the dimensionless vorticity component normal to the x-y plane:

$$\nabla^2\psi=\zeta \qquad (2)$$

$$\frac{\partial\zeta}{\partial t}+u\frac{\partial\zeta}{\partial x}+v\frac{\partial\zeta}{\partial y}=\frac{1}{R_e}\nabla^2\zeta \qquad (3)$$

in which $R_e=\Gamma'/\nu\equiv$Reynold number, ν, the kinematic viscosity and ∇^2 denotes the Laplace operator in x- and y-directions.

The contour of the barrier in this study is considered as an elliptical cylinder with length of the major axis ℓ. On this surface, boundary conditions are prescribed, according to the no-slip requirement, such that the velocity vector is zero. The dimensionless velocity components u and v are related to ψ by the equations

$$u=\frac{\partial\psi}{\partial y},\quad v=-\frac{\partial\psi}{\partial x} \qquad (4)$$

Thus, at the body surface the boundary conditions are

$$u=\frac{\partial\psi}{\partial y}=0,\quad v=-\frac{\partial\psi}{\partial x}=0 \qquad (5)$$

While at the unbounded region, the flow field is assumed to be not influenced by the interaction of the elliptical barriers, so the stream function ψ and the vorticity ζ remain invariant. The initial condition is obtained from the statement that the impulsive start of the development of flow past an obstacle can be treated as potential flow (see, for example, Batchelor 1967). The initial stream function is, therefore set as

$$\psi=\frac{U_0\ell}{\Gamma'}(y\cos\alpha-x\sin\alpha)-\ell nr \qquad (6)$$

where $r=z-a$; a, the location of stationary vortex and α is the angle of incidence of uniform flow relative to the x-axis.

3. Numerical Analysis

The infinite domain of integration in the x, y plane is replaced by a finite network of points. The differential equations are replaced by difference equations involving the values of the variables at these grid points. The computation domain is divided into 31×31 square meshes with mesh size $d\times d$, where $d=\ell/m$, m is the number of meshes occupied by the major axis of the elliptical barrier. Grid cells are half size denser near the barrier and the fixed vortex in order to resolve the higher vorticity and stream function gradients. Equation (3) yields, when solved for $\zeta_{i,j}$ at the $(n+1)$th time step, the system of finite difference equations

$$\zeta^{n+1}_{i,j}=\zeta^n_{i,j}-\Delta t(ZUC_{i,j}+ZVC_{i,j})+\frac{\Delta t}{R_e d^2}(\zeta^n_{i+1,j}+\zeta^n_{i-1,j}+\zeta^n_{i,j+1}+\zeta^n_{i,j-1}-4\zeta^n_{i,j}) \qquad (7)$$

where the terms of ZUC and ZVC correspond to the convective terms $\partial(u\zeta)/\partial x$ and $\partial(v\zeta)/\partial y$ respectively in equation (3).

To preserve the stability of the numerical scheme in the calculation of the convection $\partial(u\zeta)/\partial x$ and $\partial(v\zeta)/\partial y$ for larger Reynolds number, the non-linear space derivatives are approximated with special three point non-central differences (Torrance & Rockett 1969). The special forms are

$$\frac{\partial(u\zeta)}{\partial x}_{i,j}=ZUC_{i,j}=\frac{1}{d}\left(\frac{u_{i+1,j}+u_{i,j}}{2}\zeta_{i,j}-\frac{u_{i,j}+u_{i-1,j}}{2}\zeta_{i-1,j}\right) \qquad (8a)$$

when the coefficients $\frac{1}{2}(u_{i+1,\,j}+u_{i,\,j})$ and $\frac{1}{2}(u_{i,\,j}+u_{i-1,\,j})$ are positive and

$$\frac{\partial(u\zeta)}{\partial\zeta}_{i,\,j}=ZUC_{i,\,j}=\frac{1}{d}\left(\frac{u_{i+1,\,j}+u_{i,\,j}}{2}\zeta_{i+1,\,j}-\frac{u_{i,\,j}+u_{i-1,\,j}}{2}\zeta_{i,\,j}\right) \tag{8b}$$

when the coefficients are negative. When the mean velocities $\frac{1}{2}(u_{i+1,\,j}+u_{i,\,j})$ and $\frac{1}{2}(u_{l,\,j}+u_{l-1,\,j})$ are of different sign, a mixed expression is required which contains one term from each of equations (8), as appropriate. A similar procedure is used to approximate $\partial(v\zeta)/\partial y$ according to the sign of $\frac{1}{2}(v_{i,\,j+1}+v_{i,\,j})$ and $\frac{1}{2}(v_{i,\,j}+v_{i,\,j-1})$. The velocity components $u_{i,\,j}$ and $v_{i,\,j}$, using central difference, are

$$u_{i,\,j}=\frac{1}{2d}(\psi_{i,\,j+1}-\psi_{i,\,j-1}),$$

$$v_{i,\,j}=\frac{-1}{2d}(\psi_{i+1,\,j}-\psi_{i-1,\,j}) \tag{9}$$

Equation (2) is approximated by a five-point formula which yields for $\psi_{i,\,j}$

$$\psi_{i,\,j}=\frac{1}{4}(\psi_{i+1,\,j}+\psi_{i-1,\,j}+\psi_{i,\,j+1}+\psi_{i,\,j-1}-d^2\zeta_{i,\,j}) \tag{10}$$

The system of algebraic equations (10) is solved by the method of sequential relaxation with an over-relation factor, $E=1.4$. The iteration process is halted after the kth iteratation if

$$|\nabla^2\psi^k-\zeta^k|<\varepsilon \tag{11}$$

at each grid point, where ε is of order 10^{-3}. The number of iterations depends on the nature of the flow field.

The wall vorticity is an extremely important evaluation. The vorticity transport equation (3) for $\partial\zeta/\partial t$ determines how ζ is advected and diffused, but the total ζ is conserved at interior points. At the body surface a one-sided difference scheme must be used in order to calculate the vorticity ζ_b. Using the Taylor series expansions with the no-slip conditions and regardless of the wall orientation or boundary value of ψ, we can write the first-order approximation as

$$\zeta_b=\frac{2(\psi_{b+1}-\psi_b)}{\Delta h^2}+0(\Delta h) \tag{12}$$

where Δh is the distance from $(b+1)$ to (b), normal to the wall. For ψ_b, the stream function around the elliptical barrier is determined from the average of the initial values of ψ evaluated from equation (6) on the grid points in which the barrier is to be occupied. At the outer boundaries, the following prescribing conditions as mentioned previously are specified as

$$\partial\zeta/\partial x=0 \tag{13a}$$

on vertical outer boundaries,

$$\partial\zeta/\partial y=0 \tag{13b}$$

on horizontal outer boundaries and

$$\partial\psi/\partial t=0 \quad \text{on outer boundaries.} \tag{14}$$

The integration process is carried out in the following way. The flow is considered to be started impulsively within an infinitesimal time interval. Thus at $t=0$, the motion is assumed irrotational except at the center of the vortex. The initial flow is then obtained from the calculation of ψ_b and appropriate boundary conditions incorporated in solving the Laplace equation $\nabla^2\psi=0$. The vorticity $\zeta_{i,j}^{n+1}$ for the advanced time step $n+1$ is computed at the interior points according to equation (7). $\psi_{i,j}^{n+1}$ is then calculated with the aid of equation (10). The cycle concludes with the calculation of ζ_b^{n+1} from equation (12).

Computations were carried out in single precision on a CDC-CXBER-72 computer. The graphic display of streamlines was produced with a CNTR 2 subroutine.

4. Results and Discussion

The flow problem of a uniform flow associated with a fixed vortex in the upstream of a two-dimensional elliptical barrier has been studied numerically. The numerical results show that both of the uniform flow and the fixed vortex play important roles on the effect of flow features. The dimensionless velocity of uniform flow, $U_0\ell/l'$, is incorporated with the Reynolds number, l'/ν, to study the flow problem. As the value of $U_0\ell/l'$ is small (say, 0.5 for example), the combinated flow acts as a fixed vortex in the interaction with a barrier. Otherwise (say, $U_0\ell/l'=1.5$ for example), the steering flow plays an important role in studying

the interaction characteristics. Based on the position of fixed vortex and the angle of incidence as sketched in Fig. 1, the results are presented as follows.

(1) Case 1—fixed vortex located on x-axis.

To study the flow patterns associated with a fixed vortex in this location, Reynolds number, l'/ν, in a range of 10^2 to 10^4 was investigated in a sequence calculations. For $U_0\ell/l'=0$ and $R_e=100$; the flow around the elliptical barrier due to the fixed vortex is weak. The result shows that the streamline pattern has reached a almost steady state solution at $t=0.4864$. The flow pattern shown in Fig. 2 is quite similar to the case of Stokes flow. Fig. 3 is the flow pattern for R_e increasing to 500. It can be seen that as the fluid flow of the fixed vortex becomes faster, it migrates the stagnation point of the lower one from the midway toward the edge A of barrier and the flow has a tendency to be separated at that tip. When the

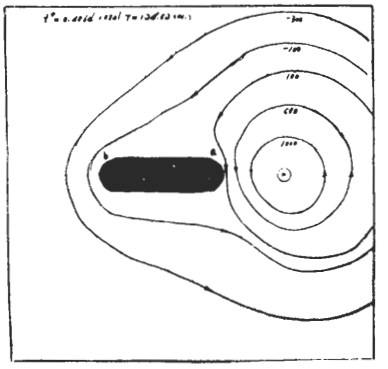

Fig. 2. Streamlines around the barrier in a fixed vortex flow for $R_e=100$ at $t=0.4864$ (125 sec).

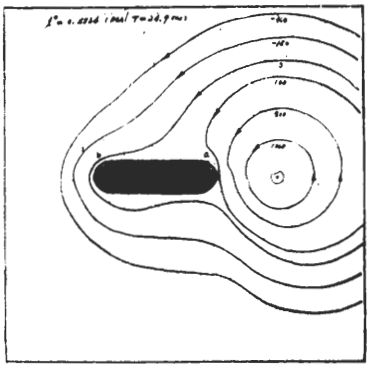

Fig. 3. Streamlines for $R_e=500$ at $t=0.4864$ (25 sec).

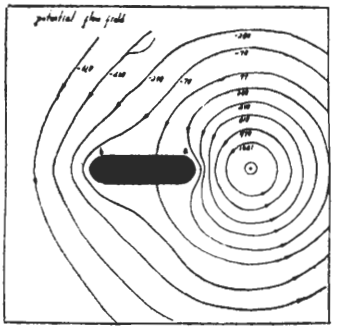

Fig. 4. (a)

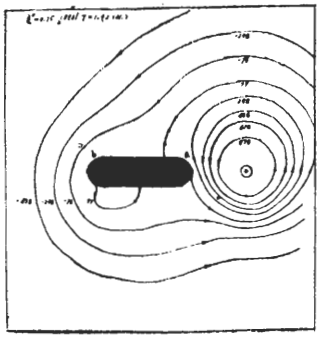

(b)

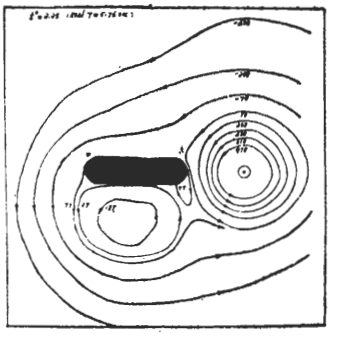

(c)

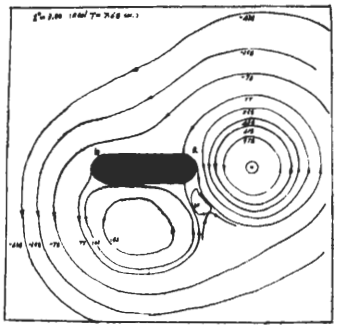

Fig. 4. (d)

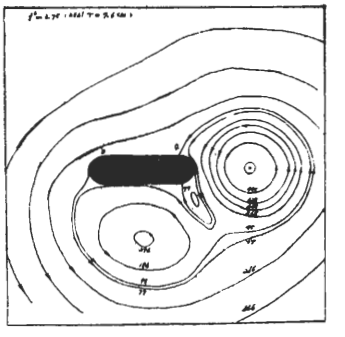

(e)

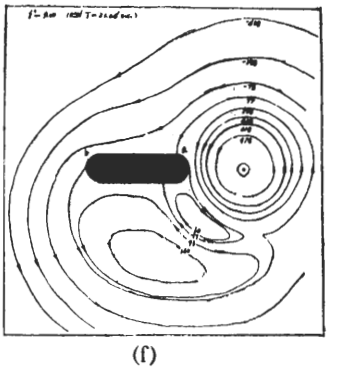

(f)

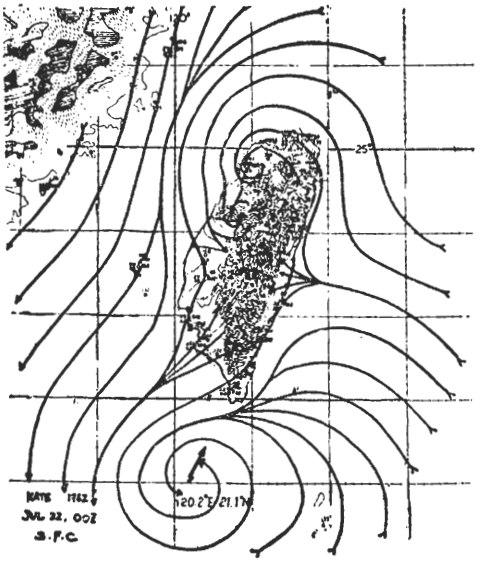

Fig. 4 (g)

Fig. 4. Some patterns of streamlines for $R_e=10^4$ at varsovs times. Potential flow at $t=0$. $t=0$.

	(a)	(b)	(c)	(d)	(e)	(f)
t	0	0.75	2.25	3.00	3.7	59.0

(q) Surface flow lines of typhoon kate, July 22, 1962.

Reynolds number is increased to 10^4, the fluid of the fixed vortex flow around the barrier becomes fast and flow seperation occurs at both tips of the barrier. An induced eddy is formed observably first at the edge B and grows with time. As this eddy grows, it tends to shed away from the barrier. This can be seen from Fig. 4. When the first eddy at edge B is shedd-

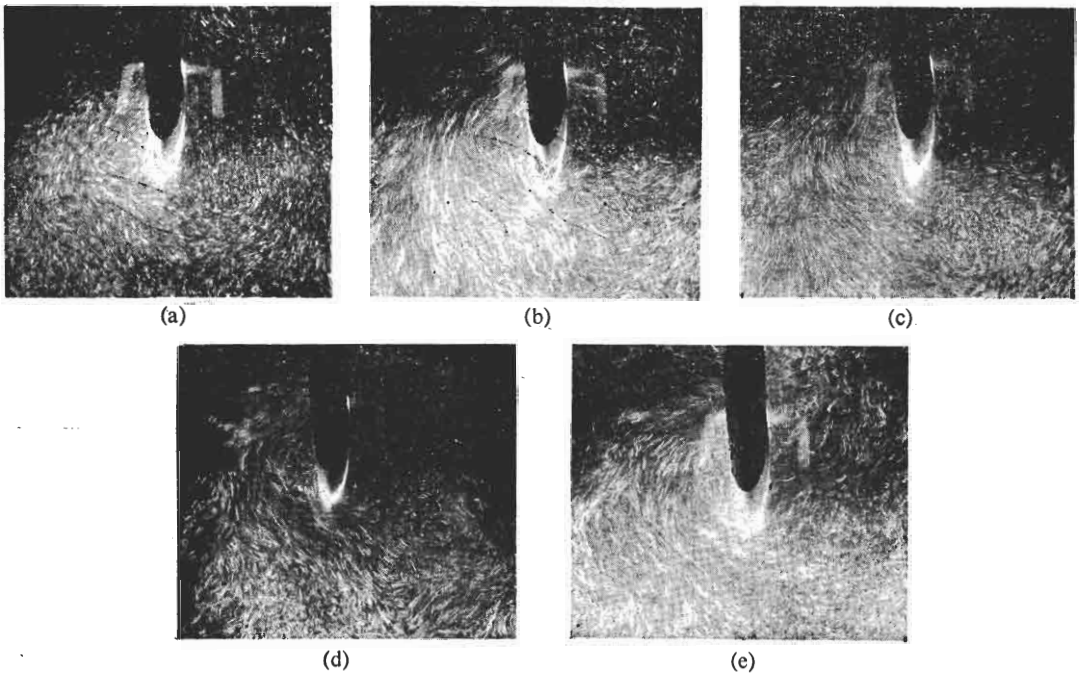

Fig. 5. Sequence of streamline pictures showing the flow pattern of the fixed vortex in the presence of an elliptical barrier. Experimental Conditions: $\Omega=16.4$ rad/sec; $U=0$; $\Omega_0=1.7$ cm; $R_e=4{,}680$; flow development at t_0.

	(a)	(b)	(c)	(d)	(e)
t	t_0+3 sec	t_0+7 sec	t_0+11 sec	t_0+15 sec	t_0+19 sec

ing, a second eddy is starting to form near the edge A. The eddy near the edge A has a tendency to grow in size and to shed away from the tip. For the purpose of comparison, surface flow lines of typhoon Kate, 1962 was analyzed and plotted in Fig. 4g. It is seen that the resemblance of the flow pattern between the numerical computations and the field data is striking. This fact was also confirmed in the experimental observation as shown in Fig. 5. When the second eddy of edge A has been shed, the eddy near edge B has closed the shedding and become full-grow, and tends to shed away again. This completes a full cycle of which commences with the shedding of a eddy from the edge B and ends with the shedding of the next time at this same edge. The alternate shedding process approaches a steady state at $t=6$ has a time interval of 1.5 between two successive cycles.

For the flow of $U_0\ell/\Gamma=1.5$, $\alpha=10^3$, the flow pattern in the interaction with a barrier is quite different from the flow described above. Owing to the effect of steering flow, an induced eddy is formed firstly at the edge A and grows with time. While the eddy is shedding, a second eddy is starting to form near the edge B. At dimensionless time $t=1.8$, both of eddies at edges A and B are shedding and growing in size. A sequence of streamlines for this flow condition can be seen in Fig. 6. In Fig. 7 the sequence of streamlines is shown for the same flow conditions except angle of incidence $\alpha=30°$.

(2) Case 2—fixed vortex located on position 2.

For flow of $U_0\ell/\Gamma=0.5$, $\alpha=0°$ and $R_e=5\times10^3$, since the steering flow is comparatively small with respect to the vortex flow, the flow feature is dominated by the effect of the fixed vortex. As shown in Fig. 8, an induced eddy is formed at first near edge B and grows with time. A second eddy is starting to form at tip A when the eddy of edge B is shedding. These two eddies are growing in size in the transient phase. The alternate phenomena of the formation and shedding of eddies at both tips is not observable in this flow condition. These results

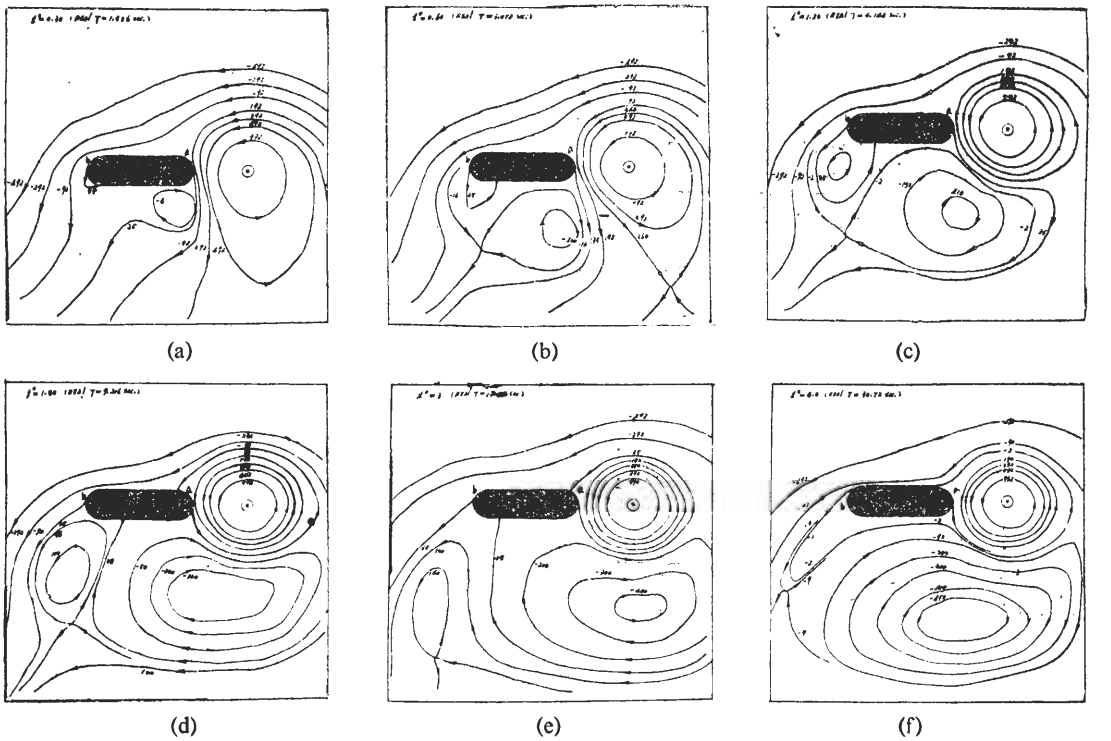

Fig. 6. Sequence of streamlines for $R_e=5\times10^3$, $U_0\ell/\Gamma=1.5$, $\alpha=0°$ at various times. Potential flow at $t=0$.

	(a)	(b)	(c)	(d)	(e)	(f)
t	0.3	0.6	1.2	1.8	3.0	6.0

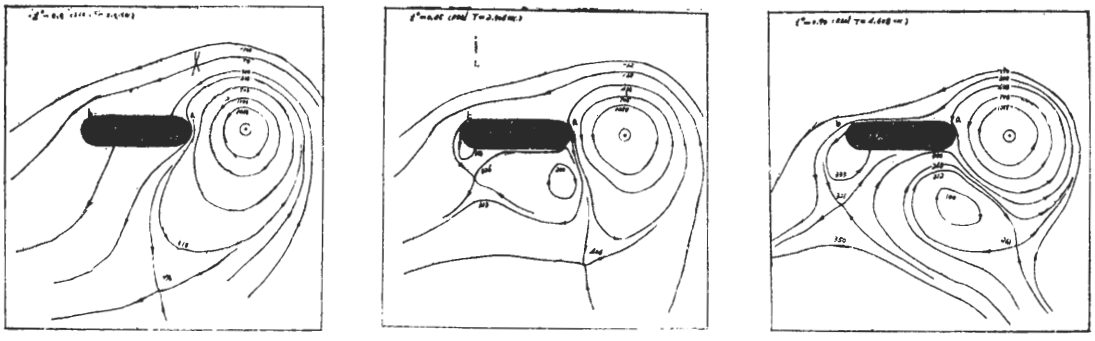

(a) (b) (c)

Fig. 7. Some patterns of streamlines for $R_e=5\times10^3$, $U_0\ell/\Gamma=1.5$, $\alpha=30°$

	(a)	(b)	(c)
t	0	0.45	0.9

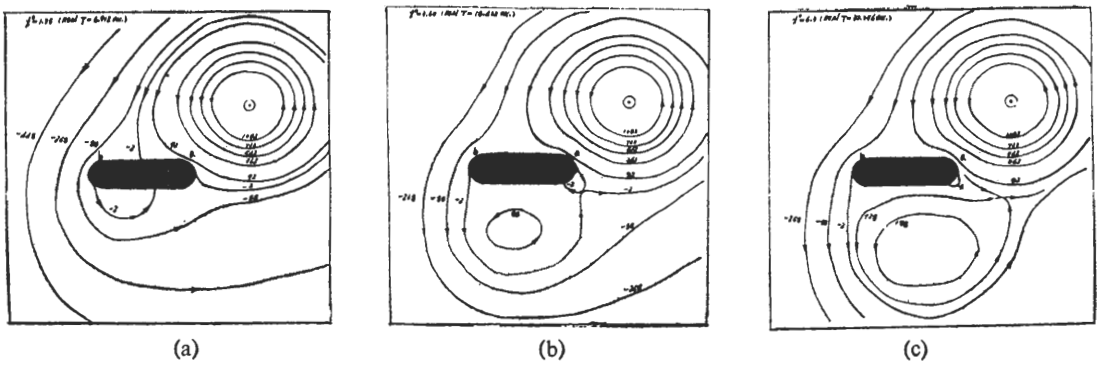

(a) (b) (c)

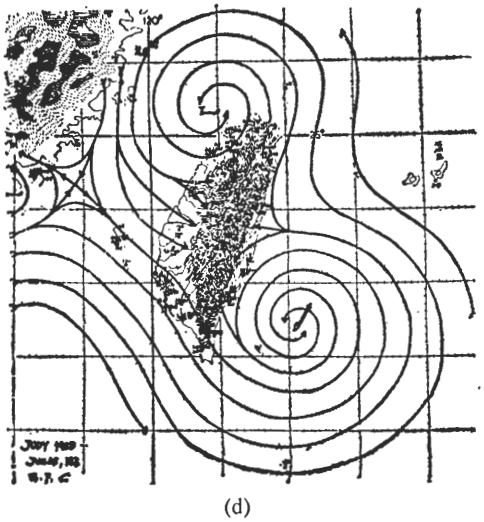

(d)

Fig. 8. Sequence of streamlines for $U_0\ell/\Gamma=0.5$, $\alpha=0°$, fixed vortex located atposition 2 at various times. Potential flow at $t=0$.

	(a)	(b)	(c)
t	1.35	3.6	6.3

(d) Surface flow ilnes of typhoon Judy, June 5, 1953.

were compared with surface flow lines of typhoon Judy, 1953 as shown in Fig. 8d. It can be seen that the agreement is remarkable. Fig. 9 shows the similar flow feature for the case of $R_e=2\times10^4$, $U_0\ell/\Gamma=0.2$ and $\alpha=30°$. These transient developments of flows can be confirmed from the pictures of experimental performation shown in Fig. 10. Fig. 11 shows the flow develodment for the case of $U_0\ell/\Gamma=1.5$, $\alpha=0°$ and $R_e=5\times10^3$. This flow feature is similar to the flow pattern as shown in Fig. 6, an eddy is formed firstly at edge A. As the eddy is shed-

ding a second eddy is starting to formed near edge B. These two eddies are then kept growing with time.

5. Conclusion

In the present study, a numerical scheme is used to analyze the flow feature of a uniform flow associated with a fixed vortex in the interaction of a two-dimensional elliptical barrier. With the numerical calculation for several flow conditions, we now make the following tentative conclusions:

(1) Induce eddies are occurred in the wake region behind the barrier. When the fluid of the vortex flow around the barrier is small, the flow is similar to Stokes flow.

(2) When the steering flow is relatively small in the combined flow field of uniform flow and fixed vortex, an induced eddy is formed observably at first near edge B. Other-

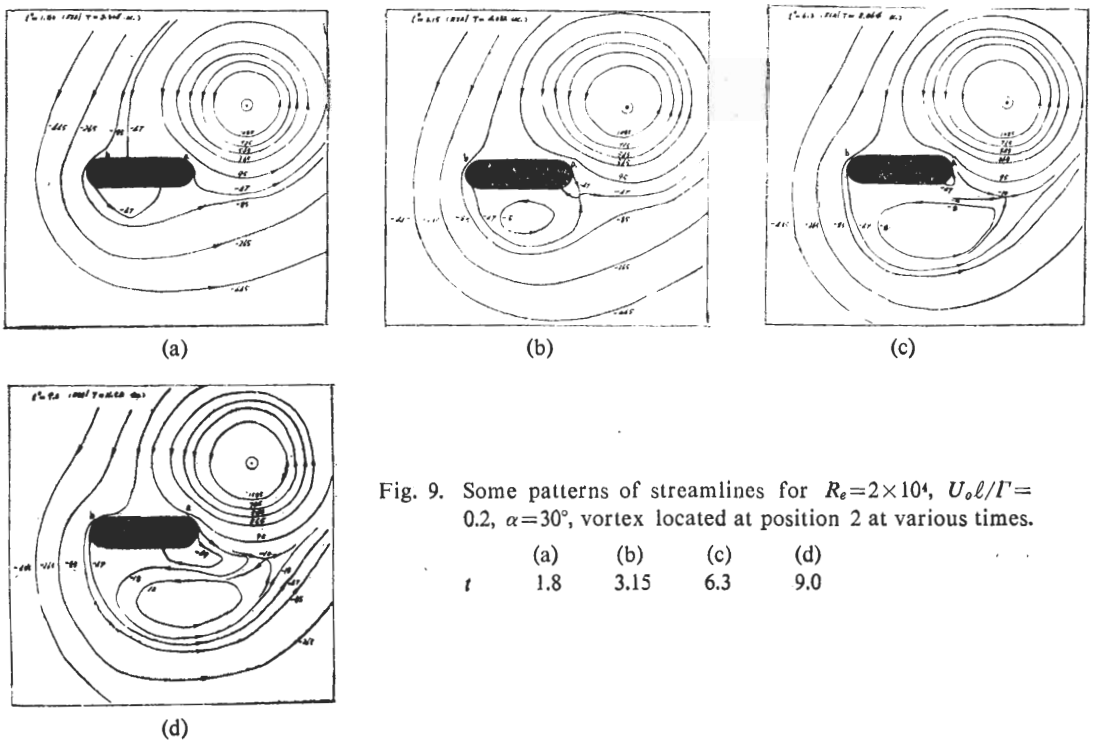

(a) (b) (c) (d)

Fig. 9. Some patterns of streamlines for $R_e=2\times10^4$, $U_o\ell/\Gamma=0.2$, $\alpha=30°$, vortex located at position 2 at various times.

	(a)	(b)	(c)	(d)
t	1.8	3.15	6.3	9.0

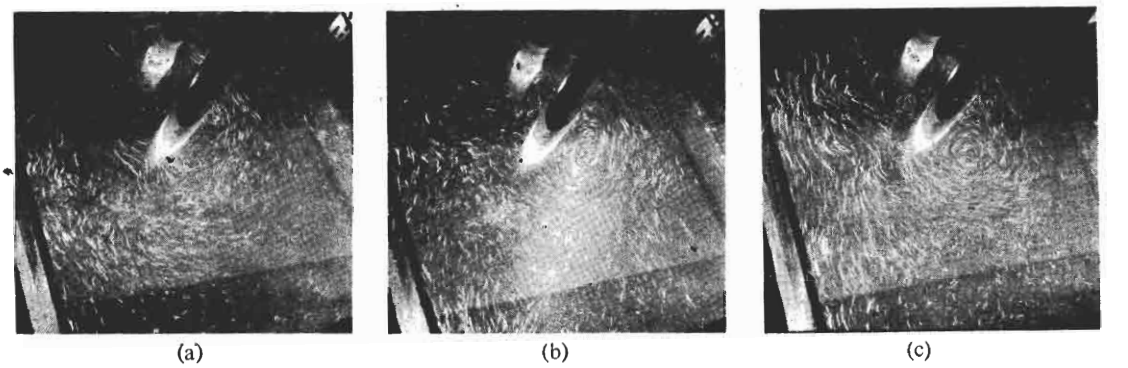

(a) (b) (c)

Fig. 10. Sequence of streamline pictures of laboratory experiment. Same experimental condions as Fig. 5, except fixed vortex located at position 2.

	(a)	(b)	(c)
t	t_o+4sec	t_o+8 sec	t_o+12 sec

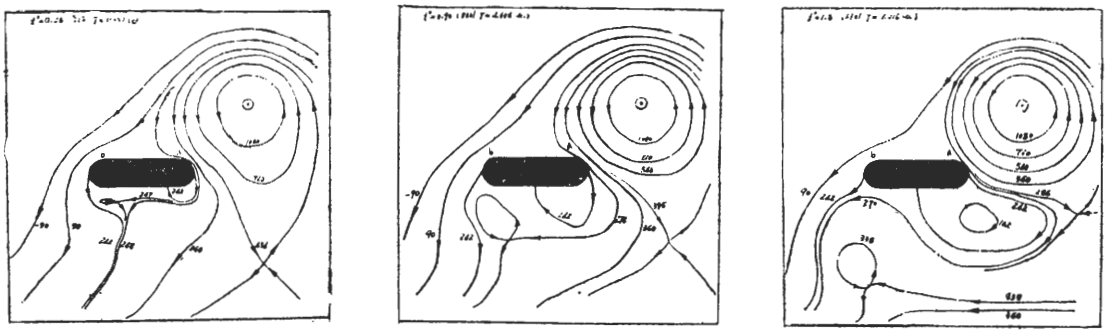

(a) (b) (c)

Fig. 11. Some patterns of streamlines for numerical results. Same flow flow conditions as Fig. 8. except $U_o\ell/\Gamma=1.5$. Potential flow at $t=0$.

	(a)	(b)	(c)
t	0.45	0.9	1.8

wise, the induced eddy will be formed near edge A. Both of induced eddies are growing in size and shedding away in the sense of transient development.

(3) For the flow of a fixed vortex, two induced eddies behind barrier will be formed and shed in an alternate development. This exchange process will be approached to a steady situation.

(4) Even the induced eddy is shedding, there will be existed stagnation point in the flow field.

Acknowledgments. This work was supported by the National Science Council of ROC and the Institute of Physics, Academia Sinica. The computer calculations were carried out on the CDC-CYBER-72 computer of Chung-Shan Institute of Science and Technology.

REFERENCES

BATCHELOR, G. K., 1967 *An Introduction to Fluid Mechanics*, London, Cambridge University press, 615pp.

BERGER, E. & WILLE, R.. 1972: Periodic flow phenomena. *Ann. Rev. Fluid Mech.*, **4**, 313-340.

CERALD, D., 1972: *Applied Numerical Analysis.* Addison Wesley Publishing Company, 340pp.

HOCKNEY, R. W., 1970: The potential calculation and some applications. *Methods in Comp. Phys.* **9**, 135-148.

LUGT, H. J. & HAUSSLING, H. J., 1974: Laminar flow past an abruptly accelerated elliptic cylinder. *J. Fluid. Mech.*, **65**, 711-734.

MITCHELL, A. R., 1971: *Computational Methods in Partial Differential Equations.* The Univ. of Dundee, Scotland. 214 pp.

PAO, H. P., 1976: The effects of mountains on a typhoon vortex as identified by laboratory experiment. Atmospharic Sciences (Meteor. Soci. of R. O. C.) 3, 55-66.

SMITH, G. D., 1971: *Numerical Solution of Partial Equations.* Brunel College of Advanced Technology, London. 251 pp.

TORRANCE, K. E. & POCKEET, J. A., 1969: Numerical study of natural convection in an enclosure with localized heating from below. *J. Fluid Mech.*, **36**, 33-54.

二維固定渦流流場遇阻之數值分析

黃榮鑑 鮑咸平 郭純園

中央研究院物理研究所 美國天主教大學

摘 要

本文以理論分析探討一固定二維渦流受阻的流場流態。利用數值方法，由流函數方程及渦度擴散方程以獲得遇阻時流場之流形變化。討論之流體爲不可壓縮之黏滯流體，受阻之起始流場爲勢能流。計算結果顯示，流形的變化與主流之流速、方向，渦旋之强度及其位置有關，並將部分之計算結果與實驗結果及實際資料比較，流場之流形變化甚爲吻合。